Afdelingen for Bærende Konstruktioner
Department of Structural Engineering
Danmarks Tekniske Højskole · Technical University of Denmark

UNIAXIAL STRESS–STRAIN CURVES OF HIGH STRENGTH CONCRETE

NICHOLAUS HOLKMANN OLSEN

Serie R No 232 1990

UNIAXIAL STRESS-STRAIN CURVES OF HIGH STRENGTH CONCRETE

NICHOLAUS HOLKMANN OLSEN

Uniaxial Stress-Strain Curves of High Strength Concrete
Copyright © by Nicholaus Holkmann Olsen 1990
Tryk:
Afdelingen for Bærende Konstruktioner
Danmarks Tekniske Højskole
Lyngby
ISBN 87-7740-052-6

PREFACE

This report has been prepared as one part of the thesis required to obtain the degree of "teknisk licentiat", equivalent to the Ph.D. degree. This thesis consist of this report and the following three reports:

- Heat-Induced Explosion in High Strength Concrete.

- Design Proposal for High Strength Concrete Sections Subjected to Flexural and Axial Loads.

- The Strength of Overlapped Deformed Tensile Reinforcement Splices in High Strength Concrete.

The thesis has been carried out at the Department of Structural Engineering, Technical University of Denmark under the supervision of Lecturer, M.Sc. Erik Skettrup, Lecturer, Dr. Herbert Krenchel and Professor Emeritus, Dr. Troels Brøndum-Nielsen.

I wish to express my sincere thanks to:

Professor Vagn Askegård, Torben Arnbjerg-Nielsen, M.Sc. and Henrik Christensen M.Sc. for their support in the construction of the test rig.

Mogens Bo Sørensen, M.Sc., who as a part of his thesis, carried out several test series in order to determine stress-strain curves for high strength concrete, and to Mona Nielsen, B.Sc., who obtained stress stress strain curves not only for high strength concrete but also for normal strength concrete.

Finally I wish to acknowledge the financial support of the Danish Technical Research Council Contract No.: FTU 5.17.3.6.11 without which it had not been possible to carry out this research.

ABSTRACT

The thesis deals with the following four investigations:

- Heat-Induced Explosion in High Strength Concrete.
- Uniaxial Stress-Strain Curves of High Strength Concrete.
- Design Proposal for High Strength Concrete Sections Subjected to Flexural and Axial Loads.
- The Strength of Overlapped Deformed Tensile Reinforcement Splices in High Strength Concrete.

The thesis consist of four seperate reports. A short summary of these is given below.

Heat-Induced Explosions in High Strength Concrete.

This report contains the result and description of a series of tests which have been carried out in order to evaluate the explosion risk of heat induced high strength concrete as compared to normal strength concrete.

The tests were carried out with concrete test specimens shaped as ø100 x 200 mm cylinders with a compressive strength in the range from 30 MPa to 90 MPa. The cylinders were cured in two different ways:

a: 7 days in water followed by 21 days in laboratory atmosphere (20^{o} C and 60 % RH).

b: 7 days in water followed by 21 days sealed with plastic aluminum foil.

A total of 36 concrete cylinders were heated in an electrical oven at a heating rate of 2.5° C per min. until reaching a temperature of 600° C. After 2 hours at this temperature the cylinders were cooled at a rate of up to 1° C per min.

The tests show that the explosion risk depends on the curing conditions and that the explosion risk in the case of high strength concrete is not higher than for normal strength concrete especially for concrete cured under condition a.

Uniaxial Stress-Strain Curves of High Strength Concrete.

This report describes a special test-rig developed in order to obtain the ascending as well as the descending part of uniaxial stress-strain curves. Test results is reported from test series where the complete stress-strain curve is determined for concrete with compressive strength in the range from 40 MPa to 92 MPa.

The test results show that the ascending part of the uniaxial stress-strain curves are more linear and steeper for high strength concrete when compared to normal strength concrete and that the descending branch becomes steeper the higher the strength level.

The inclination of the ascending part of the obtained uniaxial stress-strain curves for high strength concrete is steeper and the strain at peak stress is less when compared to results from USA and Norway. The declination of the descending part seems less when compared to the results from Norway and only slightly steeper when compared to results from USA.

Design Proposal for High Strength Concrete Sections Subjected to Flexural and Axial Loads.

In this report an investigation is carried out of the consequences when predicting the ultimate capacity of reinforced high strength concrete sections subjected to pure bending or combined bending and axial load by extrapolating DS 411 to the compressive strength level of 90 MPa. The investigation is based on calculated results using obtained knowledge of the complete uniaxial stress-strain curves for concrete and applying nonlinear computerized methods.

The investigation show that extrapolation of DS 411 overestimates the ultimate capacity of reinforced high strength concrete sections when subjected to pure bending with as much as 33 %, while DS 411 in the case of sections subjected to combined bending and axial load overestimates the ultimate capasity with as much as 39 %.

A design proposal is suggested for calculating the ultimate capacity of high strength concrete sections subjected to pure bending or combined bending and axial load. The design proposal is based on the same principles as DS 411 and the results from the nonlinear calculations using the knowledge of the complete uniaxial stress-strain curves as mentioned above.

The curvature ductility of single reinforced high strength concrete sections compared to normal strength concrete sections is also investigated on the basis of results from the nonlinear calculations. The investigation show that the ductility of high strength concrete sections is less than the ductility of normal strength concrete sections regardless of the reinforcement degree and that it can be reduced to as much as 78 %.

The Strength of Overlapped Deformed Tensile Reinforcement Splices in High Strength Concrete.

This report decribes a test series carried out in order to evaluate the strength of overlapped tensile splices in high strength concrete and the anchorage strength of deformed bars in pull-out test specimens similar to that of DS 2082.

The influence of concrete compressive strength, splitting strength and fracture energy, G_F, on the strength of overlapped tensile splices is evaluated on the basis of 22 tests. The test indicate that the fracture energy of concrete appears to be a more governing property to the strength of splices than the compressive strength and splitting strength.

The results from the tests with overlapped splices is compared to the Danish Code of Practice for the use of Concrete, DS 411. The comparison show that extrapolating DS 411 for the design of overlapped splices in high strength concrete will yield more conservative results than in the case of normal strength concrete.

The results from the tests with overlapped splices have also been compared to estimated values from a theoretical model developed at the Department of Structural Engineering by B. S. Andreasen. The model is based on the theory of plasticity and tests with concrete in the normal strength range. The comparison show that the model developed by Andreasen overestimates the strength of overlapped splices for high strength concrete. A modification to the ν-expression used in the model is suggested, yielding more acceptable deviations from the test results.

Estimated values from an empirical formula developed by Orangun et al. is compared to the results from the tests with overlapped splices. The comparison show that the empirical formula overestimates the strength of overlapped splices in high strength concrete.

The influence of concrete compressive strength, splitting strength and fracture energy, G_F, on the anchorage strength of deformed bars in pull-out test specimens is evaluated on the basis of 84 tests. No clear conclusion could be made from the tests regarding which proporty were the most governing on the anchorage strength.

A model is suggested for calculating the anchorage strength of deformed bars in pull-out test specimens similar to that of DS 2082. The model is based on the theory of plasticity as well as the experimental results and the principles used by Andreasen in his model for estimating the strength of overlapped splices.

The results from the tests with overlapped splices and pull-out tests are compared. The comparison indicates that the anchorage strength from the pull-out tests are considerably larger than the strength from overlapped splices regardless of the concrete compressive strength level. The reason for this is partly the surrounding spiral reinforcement in the pull-out test specimen which confine the concrete around the anchored bar and that the failure mechanism is completely different from that of overlapped splices.

RESUME

Afhandlingen omhandler følgende undersøgelser af højstyrkebeton:

- Heat-Induced Explosion in High Strength Concrete.

- Uniaxial Stress-Strain Curves of High Strength Concrete.

- Design Proposal for High Strength Concrete Sections Subjected to Flexural and Axial Loads.

- The Strength of Overlapped Deformed Tensile Reinforcement Splices in High Strength Concrete.

Afhandlingen foreligger som fire seperate rapporter over undersøgelserne og er kort resumeret nedenfor.

Heat-Induced Explosion in High Strength Concrete.

Denne rapport indeholder resultater og beskrivelse af en forsøgsrække udført med det formål, at undersøge explosionsrisikoen af varmepåvirket højstyrkebeton i forhold til normalstyrkebeton.

Undersøgelsen omfatter betonprøvelegemer formet som ø100 x 200 mm cylindre med en trykstyrke i intervallet 30 - 90 MPa, som er hærdnet på to forskellige måder :

a: 7 dage i vand efterfulgt af 21 dage i laboratoriet ved 20° C og 60 % RH.

b: 7 dage i vand efterfulgt af 21 dage forseglet med plastik og aluminiums folie.

Ialt 36 betoncylindre blev opvarmet i en elektrisk ovn med en opvarmningshastighed på 2.5° C pr. min. op til 600° C. Efter 2 timer ved 600° C blev cylindrene nedkølet med en hastighed på maksimalt 1° C pr. min.

Forsøgene viste, at explosionsrisikoen afhænger af hærdningsforholdene, samt at risikoen for højstyrkebeton ikke er væsentligt højere end for normalstyrkebeton, specielt når disse hærdes som under a.

Uniaxial Stress-Strain Curves of High Strength Concrete.

Rapporten beskriver en specielt udviklet forsøgsopstilling, som muliggør bestemmelse af den stigende og faldende del af enaksede betonarbejdskurver.

Rapporten indeholder derudover resultater fra forsøgsrækker, hvor hele den enaksede arbejdskurve er bestemt for beton med trykstyrker i intervallet 40 - 92 MPa. De bestemte enaksede arbejdskurver af højstyrkebeton udviser i forhold til normalstyrkebeton et mere lineært og stejlere forløb af den nedadgående del.

De opnåede arbejdskurver for højstyrkebeton udviser sammenlignet med tilsvarende arbejdskurver fra USA og Norge et stejlere forløb af den stigende del af arbejdskurven, og en mindre tøjning ved maksimal spænding, mens den nedadgående del er mindre stejl sammenlingnet med de norske resultater og stejlere sammenlignet med de amerikanske resultater.

Design Proposal for High Strength Concrete Sections Subjected to Flexural and Axial Loads.

I denne rapport vurderes om beregningsmetoden i DS 411 til bestemmelse af betontværsnits bæreevne, påvirket til ren bøjning eller kombineret bøjning og normalkraft, kan ekstrapoleres til betonstyrker i intervallet 50 -90 MPa. Vurderingen er baseret på resultaterne fra en ulineær beregningsmodel, hvor der indgår både den stigende og den faldende del af eksperimentelt bestemte enaksede betonarbejdskurver fra en tidligere undersøgelse.

Bestemmes højstyrkebetontværsnits bæreevne ved ekstrapolering af DS 411 kan bæreevnen af tværsnit med balanceret armeringsgrad påvirket til ren bøjning overvuderes med op til 33 % i forhold til resultaterne fra den ulineære beregning, mens bæreevnen af tværsnit påvirket til kombineret bøjning og normalkraft kan overvuderes med op til 39 %.

Et beregningsforslag er derfor udarbejdet til bestemmelse af højstyrkebetontværsnits bæreevne påvirket til ren bøjning eller kombineret bøjning med normalkraft. Forslaget er baseret på de samme principper som DS 411 og resultater fra den ulineære beregningsmodel.

Endvidere er duktiliteten af højstyrkebetontværsnit vurderet i forhold til normalstyrkebetontværsnit på baggrund af resultaterne fra den ulineære beregningsmodel.

Resultaterne indikerer, at duktiliteten af højstyrkebetontværsnit er mindre uanset armeringsgraden af tværsnittet og kan forminskes ned til 78 % af tilsvarende normalbetontværsnit.

The Strength of Overlapped Deformed Tensile Reinforcement Splices in High Strength Concrete.

I denne rapport beskrives for både højstyrkebeton og normalstyrkebeton en eksperimentel behandling af overlapningsstøds bæreevne samt bæreevnen af forkammet armering forankret i prøvelegemer meget lig prøvelegemet efter Dansk Standard DS 2082.

Inflydelsen af betons trykstyrke, spaltetrækstyrke og brudenergi, G_F, på bæreevnen of overlapningsstød er undersøgt på basis af 22 forsøg. Undersøgelsen viser, at betons brudenergi G_F har større inflydelse på bæreevnen af overlapningsstød end betons trykstyrke og spaltetrækstyrke.

Der er foretaget en undersøgelse af muligheden for, at ekstrapolere beregningsmodellen i DS 411 til beregning af nødvendig overlapningslængde af stød til betonstyrker i intervallet 50 - 90 MPa. Denne undersøgelse viser, at DS 411 ved ekstrapolering giver mere konservative resultater af nødvendig overlapningslængde for højstyrkebeton end for normalstyrkebeton.

Resultaterne af forsøgene med overlapningsstød er sammenlignet med resultater fra en beregningsmodel udviklet på Afdelingen for Bærende Konstruktioner af B. S. Andreasen. Modellen der baseres på plasticitetsteorien og forsøg primært med betontrykstyrker i intervallet 6 - 50 MPa, overvurderer bæreevnen af overlapningsstød i højstyrkebeton. Et forslag til et andet ν-udtryk til beregningsmodellen er derfor udarbejdet.

Derudover er forssøgsresultaterne med overlapningsstød sammenlignet med resultater fra en empirisk formel udviklet af Orangun et al, der viser at den empiriske formel overvurderer bæreevnen af overlapningsstød i højstyrkebeton.

Inflydelsen af betons trykstyrke, spaltetrækstyrke og brudenergi G_F på bæreevnen af forankret armering i prøvelegemer meget lig prøvelegemer efter DS 2082 er undersøgt på basis af 84 forsøg. Det har ikke på baggrund af disse forsøg været muligt at fastslå hvilken af ovennævnte parametre, der har størst inflydelse på bæreevnen.

Et forslag til en beregningsmodel er udviklet til beregning af forkammet armerings bæreevne i prøvelegemer meget lig prøvelegemet i DS 2082. Beregningsmodellen er baseret på plasticitsteorien og de gennemførte forsøg samt principperne anvendt af Andreasen i beregningsmodellen for bæreevnen af overlapningsstød.

En sammenligning mellem de eksperimentelt fundne bæreevner af overlapningsstød og forankring af forkammet armering viser, at sidstnævnte generelt har højere bæreevne. Dette kan skyldes, at spiralarmeringen omslutter betonen hvori armeringsjernet er forankret samt, at brudmekanismen er forskellig fra brudmekanismen i overlapningsstød.

CONTENT PAGE

LIST OF TABLES PAGE

LIST OF FIGURES

NOTATIONS

The most commonly used symbols are listed below. Exceptions from the list can appear, but this will be mentioned in the text in connection to the actual symbol.

f_c	Concrete compressive strength.
h_c	Height of concrete cylinder.
h_{sb}	Height of cylindrical steel block.
h_{sc}	Height of steel column.
y	Dimensionless stress.
x	Dimensionless strain.
A_a, B_a, C_a, D_a	Constants used in a mathematical expression for the ascending part of uniaxial stress-strain curves.
A_d, B_d, C_d, D_d	Constants used in a mathematical expression for the descending part of uniaxial stress-strain curves.
D_{cc}	Diameter of the concrete cylinder.
E_c	Secant modulus of elasticity determined as the secant in uniaxial stress-strain curves from origo to 45 % of the peak stress.
E_{co}	Secant modulus of elasticity determined as the secant in uniaxial stress-strain curves from origo to the peak stress.
P_{sb}	Load applied on the cylindrical steel block.

ϵ_c	Concrete strain.
ϵ_{ci}	Concrete strain at the inflection point of the descending part of uniaxial stress-strain curves.
$\bar{\epsilon}_c$	Average concrete strain determined from four strain gauges.
ϵ_{sb}	Measured steel strain on the cylindrical steel block.
$\epsilon_{sc1}, \epsilon_{sc2}, \epsilon_{sc3}$	Measured strain on steel No. 1, 2 and 3.
ϵ_t	Strain on the Technovit capping.
σ_c	Concrete stress.
σ_{ci}	Concrete stress at the inflection point of the descending part of uniaxial stress-strain curves.

1. INTRODUCTION

1.1 Purpose of this Investigation

It is generally recognized that the shape of the ascending part of the stress strain curve for high strength concrete in uniaxial compression is more linear and steeper, the strain at maximum stress slightly higher, and the slope of the descending part steeper, when compared to the same properties of normal strength concrete.

Stress strain curves of high strength concrete were established by Wang et al [1] and Tomaszewicz [2]. They represented the test results by two different mathematical expressions and some of the results are shown in Fig. 1.1.

In both investigations it can be seen, that the slope of the curve in the post maximum stress range becomes steeper, as the compressive strength of the concrete increases, but the shape of the ascending and especially the descending part of the curves from Tomaszewicz's investigation are steeper than those of Wang et al's investigation for the same peak stress.

In order to study the stress strain curve of high strength concrete produced with Danish materials, it was necessary to develop a test rig capable of recording not only test results on the ascending branch, but also to some extent result on the descending branch.

The main purpose of this investigation was to:

1) Develop a test rig to record the stress-strain curves of high strength concrete.

2) Accomplish test series in order to obtain stress-strain curves not only of high strength concrete with compressive strength up to a level of approximately 100 MPa, but also normal strength concrete.

3) Compare the recorded stress-strain curves for high strength concrete with those of normal strength concrete.

4) Compare the results with other investigations.

2. OBTAINING THE STRESS-STRAIN CURVES

2.1 Introduction

The stress-strain curves shown on Fig. 1.1 were obtained by two different technics, Wang et al [1] loaded 75 mm x 150 mm cylindrical concrete specimens in parallel with a steel tube. The steel tube was case hardened so that its stress-strain curve became linearly elastic up to the strain of 0.006. The thickness of the tube wall was such, that the sum of the load carried by the steel tube and the concrete cylinder was always increasing. Thus there was no release of energy from the testing machine, when the concrete in the specimen started to fail.

Tomaszewicz [2] used a closed-loop testing machine, where 150 mm x 300 mm cylindrical concrete specimens could be loaded in such a way as to maintain a constant rate of strain increase and avoid unstable failure.

The only testing machines existing at the Department of Structural Engineering capable of generating stress at the 100 MPa level on a 100 x 200 mm cylindrical concrete specimen are of the conventional type. It was therefore necessary to adapt an approach similar to Wang et al's.

The next chapters describe the test-rig, the test procedure and the determination of the relationship between concrete stress and strain.

2.2 Test-Rig

2.2.1 Design Criteria and Dimensions

Figs. 2.1 and 2.2 show the structure of the test rig and its dimension. The test-rig consists of 3 parallel columns and a cylindrical steel block placed centrally between them upon which the concrete specimen is placed. Loading of the concrete specimen takes place in parallel with the 3 steel columns.

The dimensions of the test-rig was determined according to the following design criteria:

1) The maximum load capacity of the Amsler testing machine is 10 MN.

2) The steel columns and the cylindrical steel block must be linear elastic up to the maximum load applied by the testing machine during a test.

3) The sum of the load carried by the steel columns and the concrete cylinder must always increase, thus avoiding sudden release of energy due to failing of the concrete specimen under testing.

In consequence of the test results obtained by Wang et al and Tomaszewicz the following design criteria was added.

4) Possibility to obtain a stable descending part of concretes stress-strain curve, when the steepness of the falling branch is -1.0×10^5 MPa.

5) 0.006 strain in concrete must be achieved.

2.2.2 Instrumentation of Test-Rig.

All strain gauges were supplied by Hottinger Baldwin Messtechnik, Darmstadt, West-Germany.

6 mm long strain gauges of type 4 HBM, LY 11 in full bridge configuration were placed at the middle of each steel column and at the middle of the cylindrical steel block.

The full strain gauge bridge output was monitored by a Hewlett Packard 3497A Data Acquisition/control unit controlled by a Hewlett Packard 86 Computer.

2.3 Cylindrical Concrete Specimens.

2.3.1 Preparation of Specimens.

Before testing of the cylindrical concrete specimens could take place, the cylinders were grind down to a height of 197 mm ± 0.5 mm.

The cylinders were also sand blasted on the sides so that strain gauges could be mounted on a coating of araldit. The cylinders were ready for testing 24 hours after these preparations.

2.3.2 Instrumentation of Cylindrical Concrete Specimens.

Four 85 mm long strain gauges were placed on the generatixes of the concrete cylinders.

The strain gauges were produced by the Department of Structural Engineering, Technical University of Denmark, and named BT-4 600 Ω gauge.

The strain gauges on the concrete cylinders were monitored during testing, by the same equipment as described in section 2.2.2.

2.4 Procedure.

Capping both ends of the concrete cylinder with Technovit 2060 prior to a test ensured, that the machine head would apply load simultaneously to the steel columns and the concrete cylinder. The hardening of Technovit took approximately 15 min, after which the test could commence.

The load from the testing machine was applied continously so that the strain rate on the concrete cylinder were approximately 2 microstrain/second at the ascending part of the stress-strain curve. As a consequence of the expansion of the cylindrical steel block, upon which the concrete specimen is placed, the strain rate varies at the descending part of the stress-strain curve depending

on the brittleness of the concrete. In the test results presented here the strain rate were recorded to a maximum of 35 micro-strain/second, for high strength concrete with compressive strength of approximately 90 MPa.

The full strain gauge bridge output from the steel columns and the cylindrical steel block together with the four strain gauges on the concrete cylinder were monitored every 3-10 seconds during testing, until the maximum load of 9 MN was applied by the testing machine.

2.5 Determination of Concrete Stress Values.

The uniaxial concrete stress was determined by measuring the strains on the cylindrical steel block. The measured strains were converted into loads on the cylindrical steel block by a calibration curve.

The calibration curve was established prior to the tests and is shown in Fig. 2.3.

Using linear regression analysis the formula of the curve is:

$$P_{sb} = 4404.85 \times \epsilon_{sb} \qquad (2.1)$$

where:

P_{sb}: Load applied on the cylindrical steel block, in MN

ϵ_{sb}: Measured strain on the cylindrical steel block.

The uniaxial concrete stress was determined by the formular:

$$\sigma_c = \frac{P_{sb}}{\frac{\pi}{4} \times (D_{cc})^2} \qquad (2.2)$$

where:

σ_c: Uniaxial stress on the concrete cylinder, in MPa,

D_{cc}: Diameter of the concrete cylinder, in m.

Since the diameter of the concrete cylinder is 100 mm the formula (2.2) can be written as

$$\sigma_c = 560843 \times \epsilon_{sb} \qquad (2.3)$$

2.6 Determination of Concrete Strain Values.

The concrete strain was determined by two different methods.

The first was to measure the strain by monitoring the strain gauges mounted on the generatrixes of the concrete cylinder. This determination of strain was only reliable in relation to the ascending part of the stress strain curve.

The second method was by monitoring the strain gauges on the 3 steel columns together with the strain gauges on the cylindrical steel block. Based on the assumption, that a monitored strain represents the average strain of the steel column or the cylindrical steel block, the strain on the concrete cylinder can be determined by the formula

$$\epsilon_c = \frac{1}{h_c}\left(\frac{1}{3}(\epsilon_{sc1}+\epsilon_{sc2}+\epsilon_{sc3})h_{sc}-\epsilon_{sb}h_{sb}-\epsilon_t(h_{sc}-h_{sb}-h_c)\right) \qquad (2.4)$$

where:

ϵ_c : Strain on concrete cylinder

ϵ_{sc1} : Measured strain on steel column No. 1

ϵ_{sc} : " " " " " 2

ϵ_{sc3} : " " " " " 3

ϵ_{sb} : Measured strain on cylindrical steel block

ϵ_t : Strain on Technovit capping

h_{sc} : Height of steel column

h_{sb} : Height of cylindrical steel block

h_c : Height of concrete cylinder.

Assuming that

$$\epsilon_t \sim 10 \times \epsilon_c \qquad (2.5)$$

And since

h_{sc} = 552.4 mm

h_{sb} = 355 mm

h_c = 197 mm

the concrete strain can be determined on both the ascending and descending part of the stress-strain curve by the following formula:

$$\epsilon_c = 0.91609 \times (\epsilon_{sc1} + \epsilon_{sc2} + \epsilon_{sc3}) - 1.76617 \times \epsilon_{sb} \qquad (2.6)$$

2.7 Determination of the Stress-Strain Curve.

The stress values of the ascending as well as the descending branch of the stress-strain curve were determined as described in section 2.5.

The strain values represented by the ascending branch of the stress-strain curve were determined by the four strain gauges directly attached to the concrete cylinder. This way of determinating strain is more precise, than using formula 2.6 as shown in section 2.8.2.

The strain values forming the descending branch of the stress-strain curve was determined by using formula 2.6.

Although efforts were made to make the head of the testing machine apply load simultaneously to the steel columns and the concrete cylinder, strain measurements on the steel columns and cylindrical steel block showed, that this was not the case. It was therefore necessary to translate the strain values from formula 2.6 so that strain at peak stress corresponded to the strain at peak stress recorded from the strain gauges attached directly to the concrete cylinder. A more detailed description can be found in Sørensen [19].

2.8 Precision and Accuracy of the Test.

2.8.1 Introduction

The terms "precise measurement" and "accurate measurement" are used in different senses, Mørch [4], and is defined as follows.

Precise Measurement: A precise measurement is defined as the recorded measured value plus an indifinite value, often normal distributed, originating from the used equipment.

Accurate Measurement: An accurate measurement is defined as a precise measurement plus a correction value often one-sided, originating from the test conditions and specimen characteristics.

In the following chapters the precision of the measurements will be estimated when considering high strength concrete stress-strain relationships. Furthermore, the accuracy of the established uniaxial stress-strain curves will be discussed in section 2.8.3.

2.8.2 Precision of Measurement.

Using the formula of accumulating errors [4] and estimating the standard deviations of the voltage readings and gauge factors, a standard deviation of measured strains on the concrete cylinder, steel columns and steel block are determined.

By reapplying the formula of accumulating errors it is then possible to estimate the standard deviations of determined concrete strains and stresses.

If the concrete strains are determined by monitoring the four strain gauges mounted on the cylinders, the standard deviation on the average of the concrete strain $S(\bar{\epsilon}_c)$ will be:

$$S(\bar{\epsilon}_c) = 1.5 \times 10^{-6} \quad \text{when} \quad \bar{\epsilon}_c \sim 0$$

$$S(\bar{\epsilon}_c) = 12.5 \times 10^{-6} \quad \text{when} \quad \bar{\epsilon}_c = 0.0025$$

where $\bar{\epsilon}_c$ is determined as an average of four strain gauges.

If the concrete strains for high strength are determined by using formula (2.6) an estimate of the standard deviation of the concrete strain will for a 90 - 100 MPa concrete be:

$$S(\epsilon_c) = 1.9 \times 10^{-6} \quad \text{when} \quad \epsilon_c \sim 0$$

$$S(\epsilon_c) = 50.1 \times 10^{-6} \quad \text{when} \quad \epsilon_c = 0.0025$$

$$S(\epsilon_c) = 124.0 \times 10^{-6} \quad \text{when} \quad \epsilon_c = 0.0060$$

Determination of concrete stresses was described in section 2.5. Linear regression analysis of the calibration curve gives a standard deviation on the inclination of the curve. By applying the formula of accumulating errors the following standard deviations of the concrete stresses are:

$$S(\sigma_c) = 0.5 \text{ MPa} \quad \text{when} \quad \epsilon_{sb} \sim 0$$

$$S(\sigma_c) = 1.0 \text{ MPa} \quad \text{when} \quad \epsilon_{sb} = 0.00025$$

2.8.3 Accuracy of a Stress-Strain Curve

Although the measurements carried out in the tests presented here seems precise, the accuracy of the determined uniaxial stress-strain relationship may be strongly influenced by effects originating from the testing conditions and the test specimen characteristics. Some of these effects will be described in the following.

Werner [20] showed, that the influence of the type of capping material on the peak stress level is much greater in the case of high strength concrete than normal strength concrete. As an example a 25 % decrease of the peak stress was observed when using plaster as capping material compared to using high-alumina cement. Similar results were obtained by Sangha and Dhir [8]. They furthermore observed, that the shape of the stress-strain curve, especially the descending branch, is markedly affected by the confining effect, that results from the restraint on the ends of the specimen by the testing machine platters.

Neville [10] showed, that the lower the rate at which stress increases the lower the recorded peak stress. For instance if the stress rate is increased 10 times, the recorded peak stress will increase with approximately 15 %. Rasch [7] and McHenry and Schideler [8] showed similar results and concluded, that the complete stress-strain curve is affected by the strain rate. The stress-strain curve showed a more brittle behavior when the strain rate was increased.

Blanks and McNamara [21] investigated the influence of the cylinder size on the peak stress. According to this investigation the peak stress is 4 % higher when testing 100 mm x 200 mm cylinders as compared to 150 mm x 300 mm cylinders. Comparing stress-strain curves obtained on different size of cylinders will therefore not be possible without corrections.

Askegård [5] showed experimentally that the length of strain gauges in relation to the maximum aggregate size determines to which degree, the material could be characterized as homogeneous. In the test presented in this report, the length of the strain gauges were 85 mm and the maximum aggregate size was 16 mm. As a consequence of the results from Askegård the standard deviation of the measured strain on high strength concrete cylinders will be in the order of $13 \cdot 10^{-6}$ when $\epsilon_c = 0.0003$ and $120 \cdot 10^{-6}$ when $\epsilon_c = 0.003$.

Ahmad and Shah [9] discussed two experimental methods for obtaining a complete stress-strain curve of concrete in uniaxial compression, i.e. loading the concrete specimen in parallel with a steel tube similar to Wang et al [1] and using a closed-loop testing system similar to Tomaszewicz [2]. They concluded, that the first mentioned method gives very reproducible descending portions of the stress-strain curve. The stress-strain curves resulting from each testing methods showed differences in both the ascending and descending brances. When using the closed-loop testing system, changes in the size of the specimen and strain rate may result in significant changes in the descending branch and, to lesser extent, in the ascending branch.

From the references mentioned above, it can be concluded that deviations, caused by the measuring technic presented in section 2.8.2 are negligible as compared to deviations caused by effects of testing conditions and test specimen characteristics.

3. ANALYTIC EXPRESSION OF THE STRESS-STRAIN RELATIONSHIP

3.1 Introduction

Many investigations have proposed formulas for the stress-strain curve of concrete [11]. Most of these formulas have one or more of the following shortcomings:

a) they are based only on the properties of the ascending part [12] - [16],

b) they contain constants which can be changed to fit a given curve, but these constants are not based on any particular physical characteristics of the stress strain curve [17], [18]

c) the descending part does not always have an inflection point or it does not have a long descending "tail", which is characteristic for concrete behaviour [18], [4].

3.2 Proposed Analytic Expression.

Wang et al [1] found that the following expression gave the most acceptable fit to stress-strain curves of concrete:

$$y = \begin{cases} \dfrac{A_a \cdot x + B_a \cdot x^2}{1 + C_a \cdot x + D_a \cdot x^2}, & 0 \le x \le 1 \quad \text{(Ascending part)} \\ \dfrac{A_d \cdot x + B_d \cdot x^2}{1 + C_d \cdot x + D_d \cdot x^2}, & x > 1 \quad \text{(Descending part)} \end{cases}$$

where

$$y = \sigma_c / \sigma_{co}$$

$$x = \epsilon_c / \epsilon_{co}$$

σ_c and ϵ_c are stress and strain in general.

σ_{co} and ϵ_{co} are peak stress and corresponding strain.

A_a, B_a, C_a and D_a constants for the ascending part of the stress strain curve.

A_d, B_d, C_d and D_d constants for the descending part of the stress strain curve.

For the ascending part of the stress strain curve the values of the four constants are established from the following four conditions, suggested by Wang et al:

1) $\frac{dy}{dx} = \frac{E_c}{E_{co}}$, when $(y = 0, x = 0)$

where

E_c represents the secant modulus of elasticity at $0.45 \cdot \sigma_{co}$

E_{co} represents the secant modulus of elasticity at the peak stress

2) $y = 0.45$ for $x = \frac{0.45}{E_c/E_{co}}$

3) $y = 1$ for $x = 1$.

4) $\frac{dy}{dx} = 0$ for $(y = 1, x = 1)$

For the descending part of the stress strain curve the values of the four constants are established from the following four conditions, suggested by the author.

1) $y = 1$ for $x = 1$

2) $\frac{dy}{dx} = 0$ for $y = 1$, $y = 1$

3) $y = \frac{\sigma_{ci}}{\sigma_{co}}$ for $x = \frac{\epsilon_{ci}}{\epsilon_{co}}$

where σ_{ci} and ϵ_{ci} are the stress and strain at the inflection point

4) $y \to 0$ for $y \to \infty$

With this approach an analytical stress strain curve can be generated from the knowledge of three key points on the experimental curve.

1) Stress and strain at peak

2) Stress and strain at $0.45 \cdot \sigma_{co}$

3) Stress and strain at the inflection point.

4. DETERMINATION OF STRESS-STRAIN CURVE OF HIGH STRENGTH CONCRETE FROM THE FIRST TEST SERIES

4.1. Introduction.

The first test series is part of the experimental work carried out by M.Sc. Mogens Bo Sørensen in order to achieve the degree of Master of Science [19]. M.B. Sørensen investigated the influence of different aggregates on the shape of the uniaxial stress strain curve of high strength concrete, supervised by the author and Professor T.C. Hansen, The Building Materials Laboratory, Technical University of Denmark.

The stress-strain relationship of high strength concrete with compressive strength on the 90 MPa and 70 MPa level (produced with ordinary Danish aggregates) will be presented.

In the following sections the concrete used in the tests will be described. Section 4.3 presents the experimental results obtained together with the mathematical representation.

4.2 Concrete

4.2.1 Materials.

Cement: Rapid hardening portland cement, ASTM Type III, supplied by Ålborg Portland. Specific gravity was assumed to be $3.3 \cdot 10^3$ kg/m^3.

Silica Fume: Silica fume, supplied by Ålberg Portland, Ålborg. Specific gravity was assumed to be $2.2 \cdot 10^3$ kg/m^3

Fine Aggregate: Sand (0-4 mm) from Danish marine deposits, supplied by Carl Nielsen A/S, Copenhagen. Specific gravity was assumed to be $2.62 \cdot 10^3$ kg/m^3

Coarse Aggregate: Gravel (4-16) from Danish marine deposits, supplied by Carl Nielsen A/S, Copenhagen. Specific gravity was assumed to be $2.62 \cdot 10^3$ kg/m^3

Admixtures: Superplasticizer Mighty 100, supplied under the name of Scan Cem SP62/SP63 by Cemton, Norway.

Water: Tap water from the city's network was used.

4.2.2 Mix Proportions

Two different mixes were used in order to produce high strength concrete with compressive strengths of 90 MPa and 70 MPa. Mix proportions are given in table 4.1.

4.2.3 Mixing, Casting and Curing

Mixing Sand and coarse aggregates were mixed dry with cement and silica fume in a paddle mixer. After 1 min. of mixing the water and the superplasticizer were added and thorough mixing was achieved in approximately 6 min.

Casting 18 cylinders were cast from each batch in polyethylene moulds, ø 100 x 200 mm. A vibrator table was used to consolidate the concrete in the moulds.

Curing The moulds of all the cylinders from one batch were removed approximately 24 hours after casting. The cylinders were then cured for 7 days in a water basin. The continuing 21 days curing took place at 20°C and 60 % RH which is the approximate environmental condition in the test hall.

4.3 Experimental Results

4.3.1 Obtained Stress-Strain Curves

Of the 18 cylinders cast in each batch, 9 cylinders were tested in order to determine the compressive strength and 9 cylinders were tested to determine the stress-strain curve. The results of the compressive strength tests are given in Sørensen [19], together with a more detailed description of each test.

Figures 4.1 and 4.2 showes the stress-strain curves obtained from concrete specimen having a compressive strength of approximately 90 MPa and 70 MPa respectively. It can be seen that the ascending part of the stress-strain curve is considerably more "narrowed" than the descending branch, regardless of the compressive strength. Furthermore, it can be seen that the ascending part of the stress-strain curve is more linear and steeper for high strength concrete with compressive strength on the 90 MPa level, and that the strain at the maximum stress is slightly higher.

Similar results concerning the ascending part of the stress-strain curve is observed by numereous investigations and given in Carreira and Chu [3].

From the figures 4.1 and 4.2 it can be seen, that the descending part of the stress-strain curves are steeper in the case of high strength concrete with $f_c \cong 90$ MPa. It must be emphasized, that the strain rate is different on the descending part of the stress-strain curves for the two types of high strength concrete, caused by the test-rig design described in section 2.4. As a consequence the slopes of the descending parts of the stress- strain curves in the case of concrete with $f_c \cong 90$ MPa would be less, if it was possible to have the same strain rate, as when testing high strength concrete with $f_c \cong 70$ MPa.

Furthermore, it can be observed from Fig.ure 4.1 that the slope of the descending part of the stress-strain curves are close to the limitations of the test-rig, causing difficulties in observing the inflection points used when the stress-strain curves are to be represented by the mathematical expression.

4.3.2 Mathematical Expression to Represent the Stress Strain Curve.

The coordinate of the three key points mentioned in section 3.2 were determined for each stress-strain curve. As described in section 4.3.1 the inflection point of the descending part of the stress-strain curve were difficult to observe in the case of high strength concrete with $f_c \cong 90$ MPa. The inflection point of each of these stress-strain curves were therefore estimated to be on a stress level of 35 % of the peak stress.

The average values of the three key points for each concrete type are given in table 4.2 and from these values the constants in the mathematical expression were determined as described in section 3.2 and also given in table 4.2.

Figure 4.3 and 4.4 show the mathematical expression together with the experimental results, for high strength concrete with $f_c \cong 90$ MPa and $f_c \cong 70$ MPa respectively. As it can be seen from the figures, the mathematical representation of stress-strain curves fits the experimental test results quite well.

5. DETERMINATION OF STRESS-STRAIN CURVES OF HIGH - AND NORMAL STRENGTH CONCRETE FROM THE SECOND TEST SETIES

The results presented here are part of the experimental work carried out by B.Sc. Mona Nielsen employed under the Danish Technical Research Council Contract No.: FTU 5.17.3.6.11 and supervised by the author and lecturer, M.Sc. Erik Skettrup. A detailed report on the experimental results is given in [22].

The stress-strain relationship of two types of high strength concrete with compressive strength on the 90 and 70 MPa level will be presented together with two types of normal strength concrete on the 50 and 40 MPa level.

In the following section 5.2 a description of the concrete used in the tests will be given. Section 5.3 presents the experimental results together with the mathematical representation.

5.2 Concrete.

5.2.1 Materials.

Materials which were used in these test series, such as cement, silica fume, aggregates, admixtures and water were the same as described in section 4.2.1.

Fly ash supplied by Amagerværket, Copenhagen was used in the mix when producing concrete with compressive strength on the 40 MPa level.

5.2.2 Mix Proportions.

Mix proportions of the two types of high strength concretes and the two types of normal strength concrete are given in table 5.1. The mixes were designed by adjusting previous mixes used at the Department, in order to accomplish nearly constant volume ratio between sand and total amount of aggregates. Furthermore the

mixes were designed in order to obtain a constant volume ratio of paste.

By designing the mixes as described above it was possible to study the influence of f_c on the shape of the stress strain curve.

5.2.3 Mixing, Casting and Curing.

Mixing Sand and coarse aggregates were mixed dry with cement and silicafume or fly ash.

After 4 min. of mixing the water was added and after 8 min. the superplasticizer. Thorough mixing was achieved in approximately 12 min.

Casting From each batch 20 cylinders were cast in steel moulds, ø 100 mm x 200 mm, and the concrete was consolidated by the use of a vibrator table.

Curing The moulds of all the cylinders from one batch were removed approximately 24 hours after casting. The cylinders were then cured 14 days in a water bassin. The following 15-16 days of curing took place at 20°C and 60 % RH which is the environmental conditions in the test hall.

5.3 Experimental Results.

5.3.1 Established Stress-Strain Curves.

From the 20 cylinders cast in each batch, 13 cylinders were tested in order to determine the compressive strength and the ascending part of the stress-strain curve under two different stress rates. The remaining 7 cylinders were tested in order to obtain both the ascending as well as the descending part of the stress-strain curve and only the succesfully obtained stress-strain curves are presented in this report.

The obtained stress-strain curves of the two high strength concretes with $f_c \cong 90$ MPa and $f_c \cong 70$ MPa are shown in Fig. 5.1 and 5.2 respectively, while the obtained stress-strain curves of the two normal strength concretes with $f_c \cong 50$ MPa and $f_c \cong 40$ MPa are shown in Fig. 5.3 and 5.4 respectively.

Similar to what was observed in section 4.3.1, it can also here be seen from Fig. 5.1, 5.2, 5.3 and 5.4 that the ascending part of the stress-strain curves are considerably more narrow than the descending part, and that the slope of the descending branch shown in Fig. 5.1 appears to be close to the limitations of the test rig.

In Fig. 5.5 all the succesfully obtained test results are plotted and it can be seen, that the shape of the ascending part of the stress-strain curve is more linear and steeper for high strength concrete than for normal strength concrete. The descending branch seems to become steeper the higher the compressive strength of the concrete. It can also be seen, that the strain at maximum stress seems to descrease as the compressive strength increases from 40 MPa to 70 MPa, while from 70 MPa to 90 MPa the strain at maximum stress seems to increase.

5.3.2 Mathematical Expression to Represent the Stress-Strain Curve.

The coordinates of the three key points in section 3.2 is determined for each stress-strain curve. As mentioned in section 5.3.1 the declination of the stress-strain curves was close to the limitations of the test rig in the case of high strength concrete with $f_c \cong 90$ MPa. The inflection points of these stress-strain curves are therefore difficult to determine, but is estimated to be on a stress level of 35 % of the peak stress.

The average values of the three key points for each of the four concrete types are given in table 5.2. From these average key

points the constants in the mathematical expression can be calculated, and are given in table 5.2.

In Fig. 5.6, 5.7, 5.8 and 5.9 the mathematical representation are plotted against the obtained test results. As it can be seen from the figures the ascending branch of the mathematical representation fits the tests satisfactorely. The descending branch of the mathematical representation seems also to fit the test results reasonably well.

Fig. 5.10 and 5.11 show the mathematical representations of high strength concrete with $f_c \cong 90$ MPa and $f_c \cong 70$ MPa respectively, obtained from the first and second test series.

From Fig. 5.10 it can be seen, that the ascending part of the stress strain curves are nearly identical, but the peak stress level is different. The descending branches of the curves seems to be of similar shape.

Fig. 5.11 show a different slope of the ascending branch. This may have been caused by insufficient vibration during casting, and explains the softer character of the ascending part of the stress-strain curve and the more steeper shape of the descending branch.

6. RESULTS COMPARED WITH OTHER INVESTIGATIONS

6.1 Introduction

Results obtained by Wang et al [1] and Tomaszewicz [2] represents, to the authors knowledge, the only investigations covering not only the ascending but also the descending branch of the uniaxial stress-strain curve for high strength concrete. The results presented in this report represented by mathematical expression will therefore be compared to the following:

1) The mathematical representations proposed by Wang et al [1] and Tomaszewicz [2].

2) The mathematical representations proposed by CEB.

6.2 Comparison to Wang et al and Tomaszewicz

Fig. 6.1 and 6.2 show the stress-strain relationship of high strength concrete with compressive strength on the 90 MPa respectively 70 MPa level. While Fig. 6.3 and 6.4 show normal strength concrete with compressive strength on the 50 MPa respectively 40 MPa level.

The following can be seen from the figures:

1) The inclination of the ascending branch of the obtained stress-strain curves seems regardless of the compressive strength level to be more pronounced compared to the stress-strain curves obtained by Wang et al and Tomaszewicz.

2) The strain at peak stress of the present stress-strain curves seems, regardless of the compressive strength level less, when compared to Wang et al and Tomaszewicz.

3) The descending branch of the present stress-strain curves seems in general to indicate less brittleness compared to results obtained by Tomaszewicz, while the opposite is the case when compared to results obtained by Wang et al.

The differences in the stress strain curves described above may be caused by testing conditions and specimen characteristics which is described in section 2.8.3.

An explanation to why the stress-strain curves seems different is not done for the following reasons:

1) All details of the investigation accomplished by Wang et al and Tomaszewicz, concerning the test conditions and specimen characteristics are not known by the author.

2) The influence of differences in details concerning test conditions and specimen characteristics known to the author, is difficult to evaluate without data from special test series adapted to investigate the influence of these differences under controlled conditions.

6.3 Comparison to CEB-proposal.

In Fig. 6.5 and 6.6 is shown the mathematical representations of high strength concrete on the 90 MPa respectively 70 MPa level, compared to the proposal from CEB.

In Fig. 6.7 and 6.8 is shown the mathematical representations of normal strength concrete with compressive strength on the 50 MPa respectively 40 MPa level, compared to the proposal from CEB.

The following can be seen from the figures:

1) The inclination of the ascending branch of the stress strain curves presented here is, regardless of the compressive strength, steeper than the proposal from CEB. Furthermore, the strain at peak stress seems in general higher in the CEB case.

2) The descending branch of the obtained stress strain curves seems to indicate less brittleness than the proposal from CEB.

7. CONCLUSION

The following conclusions can be made from the investigation presented in this report.

1) It was possible to develop a test-rig, capable of recording not only the ascending but also the descending branch of the stress-strain curve of high strength conctrete.

2) It was observed, that the shape of the ascending part of the stress-strain curve is more linear and steeper for high strength concrete than for normal strength concrete, and that the descending branch becomes steeper the higher the compressive strength of the concrete. Furthermore, the strain at maximum stress in the case of high strength concrete with a compressive strength of 90 MPa seems only slightly higher when compared to normal strength concrete. In the case of high strength concrete with compressive strength of 70 MPa the strain at maximum stress seems slightly less when compared to normal strength concrete.

3) The inclination of the ascending part of the obtained stress-strain curves is, regardless of the compresssive strength, steeper and the strain at peak stress is less, when compared to the investigations of Wang et al [1], Tomaszewicz [2] and CEB proposal.

4) The declination of the descending part of the obtained stress-strain curves seems in general less when compared to the investigation of Tomaszewicz and the proposal of CEB, but only slightly steeper in the case of high strength concrete when compared to Wang et al.

8. REFERENCES

[1] Wang, P.T.; Shah, S.P., and Naaman, A.E., "Stress-Strain Curves of Normal and Lighweight Concrete in Compression", ACI Journal, Proceedings V. 75, No. 11, November 1978, pp. 603-611.

[2] Tomaszewicz, A, "Betonens Arbejdsdiagram", SINTEF, STF65, A84065, Trondheim, 1984.

[3] Carreira, D.J., and Chu, K., "Stress-Strain Relationship for Plain Concrete in Compression", ACI Journal, Proceedings V. 82, November 1985, pp. 787-804.

[4] Mørch, K.A. "Måleteori og Databehandling og Dimensionsanalyse", Kompendium til Laboratoriekursus i Fysik, LTF1, Technical University of Denmark, 1974.

[5] Askegård, V., "Eksperimentel Mekanik", Polyteknisk Forlag, Lyngby, Denmark, 1976, (in Danish).

[6] Shangha, C.M. and Dhir, R.K., "Strength's and Complete Stress-Strain Relationships for Concrete Tested in Uniaxial Compression under Different Test Conditions", Materials and Structures, Research and Testing (RILEM, Paris), V. 5, No. 30, Nov.-Dec. 1972, pp. 361-370.

[7] Rasch, C. "Stress-Strain Relation of Concrete and Stress Distribution in the Flexural Compression Zone at Constant Strain Rate". Bulletin No. 154, Deutsher Auschuss für Stahlbeton, Berlin, 1963, 72 pp. (in German).

[8] McHenry, Dl., and Shideler, J.J., "Review of Data on Effect of Speed in Mechanical Testing of Concrete," Symposium on Speed in Testing, SPT-185, ASTM, Philadelphia, 1956, pp. 72-82.

[9] Ahmad, S.H., and Shah, S.P., "The Complete Stress-Strain Curve of Concrete and Nonlinear Design". Progress Report, National Science Foundation Grant No. PPR 78-22878, Department of Materials Engineering, University of Illinois at Chicago Circle, Aug. 1978, 29 pp.

[10] Neville, A.M., "Properties of Concrete", Third Edition, Longman Scientific and Technical 1986, Longman House, Burnt Mill, Harlow, Essex, England.

[11] Popovics, Sandor, "A Review of Stress-Strain Relationships for Concrete", ACI Journal, Proceedings V. 67, No. 3, Mar. 1970, pp. 243-248.

[12] Popovics, Sandor, "A Numerical Approach to the Complete Stress-Strain Curve of Concrete", Cement and Concrete Research, V. 3, No. 4, Sept. 1973, pp. 583-599.

[13] Desayi, Prakash, and Krishman, S., "Equation for Stress-Strain Curve of Concrete", ACI Journal, Proceedings V. 81, No. 3, Mar. 1964, pp. 345-350.

[14] Saenz, Luis P., Discussion of "Equation for Stress-Strain Curve of Concrete" by Prakash Desayi and S. Krishnan, ACI Journal, Proceedings V. 61, No. 9, Sept. 1964, pp. 1229 and 1236.

[15] Smith, G.M. and Young, L.E., "Ultimate Flexural Analysis Base in Stress-Strain Curve of Cylinders", ACI Journal, Proceedings V. 53, No. 6, Dec. 1956, pp. 597-609.

[16] Smith, G.M. and Young, L.E. "Ultimate Theory in Flexure by Exponential Function", ACI Journal, Proceedings V. 52, No. 3, Nov. 1955, pp. 349-359.

[17] Sturman, Gerald M., Shah, Surendra P., and Winter, George, "Effects of Flexural Strain Gradients on Microcracking and Stress-Strain Behavior of Concrete", ACI Journal, Proceedings V. 62, No. 7, July 1965, pp. 805-822.

[18] Kulicki, J.M. and Kostem, C.N., "Inelastic Response of Prestressed Concrete Beams", Publications, International Association for Bridge and Structural Engineering (Zurich), V. 35-II, 1975, pp. 101-112.

[19] Sørensen, M.B., "Højstyrkebetons Deformationsforhold", M.Sc. theses, The Department of Structural Engineering and The Building Materials Laboratory, Technical University of Denmark, June 1988.

[20] Werner, G., "The effect of type of Capping Material on the Compressive Strength of Concrete", Proc. ASTM, 58, pp. 1166-81, 1958.

[21] Blanks, R.F. and McNamara, C.C., "Mass Concrete tests in large cylinders", ACI Journal, 31, pp. 280-303, Jan-Feb 1935.

[22] Nielsen, M., "Højstyrkebeton, Trykarbejdslinier", Report R 136, Department of Structural Engineering, Technical University of Denmark, Lyngby, 1988.

[23] Revision of CEB Model Code 1978, 1. Draft, Chapter 2, January 1988.

9. TABLES

Compressive strength level	90	70
Portland Rapid Cement	393	314
Silica Fume	40	31
Superplasticizer	25	14
Sand (0-4mm)	872	936
Gravel (4-8mm)	375	411
Gravel (8-16mm)	615	602
Water	103	103
Units	kg/m^3	kg/m^3

Table 4.1 Mix propertions for the concrete used in the first test series.

Compressive strength level	90	70
σ_{co} (MPa)	91.9	63.8
ϵ_{co} ($^o/oo$)	2.177	1.956
ϵ_{c45} ($^o/oo$)	0.825	0.669
σ_{ci} (MPa)	32.2	40.0
ϵ_{ci} ($^o/oo$)	3.030	2.410
A_a	1.05314	1.16652
B_a	-0.87542	-0.65543
C_a	-0.94686	-0.83348
D_a	0.12458	0.34457
A_d	0.05941	0.07339
B_d	0	0
C_d	-1.94059	-1.92661
D_d	1	1

Table 4.2 Average values of the three key points and the constants in the mathematical expression, representing the results from the first test series. ϵ_{c45} is strain at a stress level of 45 % of peak stress.

Compressive strength level	90	70	50	40
Portland Rapid Cement	393	393	365	229
Silica Fume	39	20	-	-
Fly Ash	-	-	-	90
Superplasticizer	8.5	5.1	-	-
Sand (0-4mm)	699	696	693	692
Gravel (4-8mm)	300	298	297	301
Gravel (8-16mm)	898	894	890	903
Water	109	129	146	153
Units	kg/m^3	kg/m^3	kg/m^3	kg/m^3

Table 5.1 Mix proportions for the concrete used in the second test series.

Compressive strength level	90	70	50	40
σ_{co} (MPa)	85.4	64.8	51.9	40.2
ϵ_{co} ($^o/oo$)	1.940	1.623	1.627	1.860
ϵ_{c45} ($^o/oo$)	0.803	0.643	0.558	0.510
σ_{ci} (MPa)	29.9	46.0	33.0	30.0
ϵ_{ci} ($^o/oo$)	2.762	2.190	2.580	3.150
A_a	1.08648	1.15113	1.30540	1.62818
B_a	-0.80490	-0.68222	-0.44744	-0.12031
C_a	-0.91352	-0.84887	-0.69460	-0.37182
D_a	0.19510	0.31778	0.55256	0.87969
A_d	0.06790	0.22131	0.37778	0.83619
B_d	0	0	0	0
C_d	-1.93210	-1.77869	-1.62222	-1.16381
D_d	1	1	1	1

Table 5.2 Average values of the three key points and the constants in the mathematical expression, representing the results from the second test series. ϵ_{c45} is strain at a stress level of 45 % of peak stress.

10. FIGURES

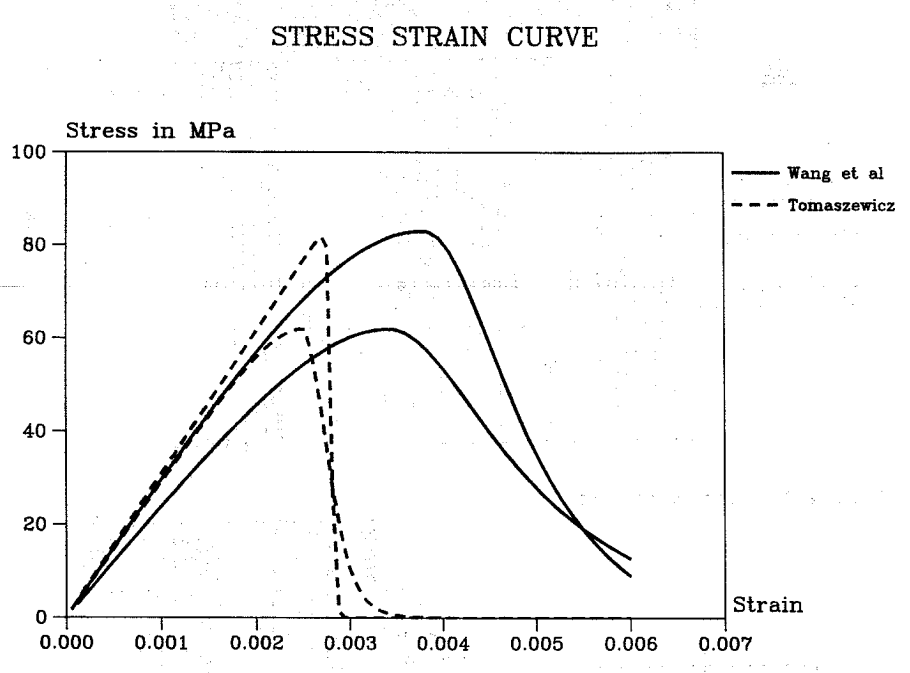

Fig. 1.1 Mathematical representation of stress strain curves obtained by Wang et al and Tomaszewicz.

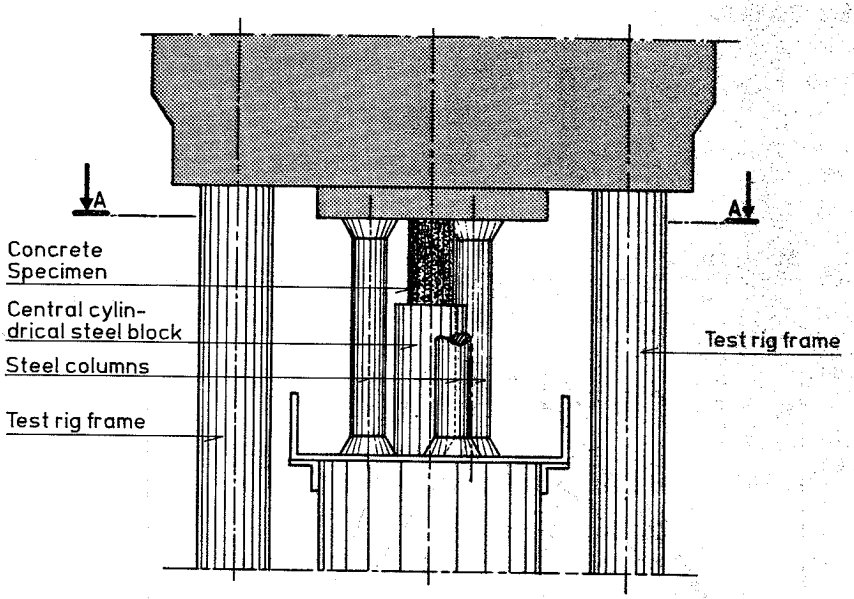

Fig. 2.1 The test rig.

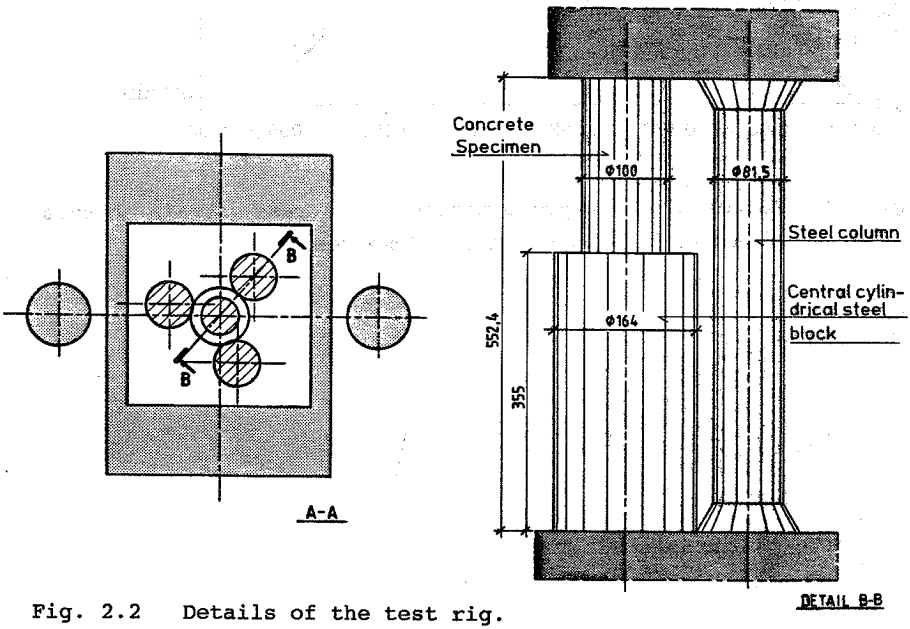

Fig. 2.2 Details of the test rig.

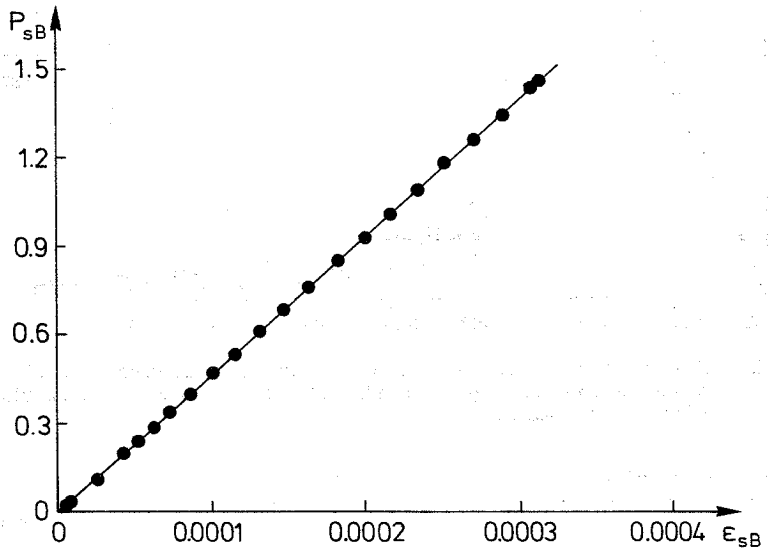

Fig. 2.3 Calibration curve of cylindrical steel block.

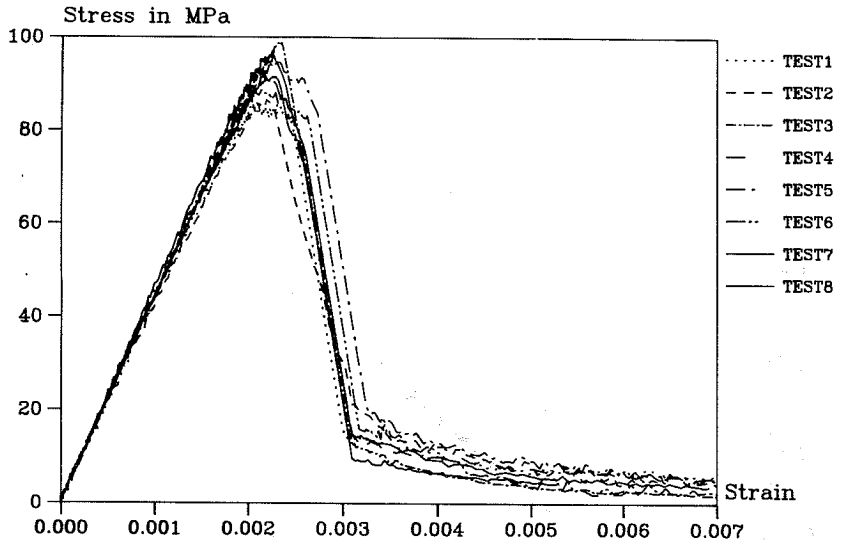

Fig. 4.1 Stress-strain curves of high strength concrete with compressive strength on the of 90 MPa level, from the first test series.

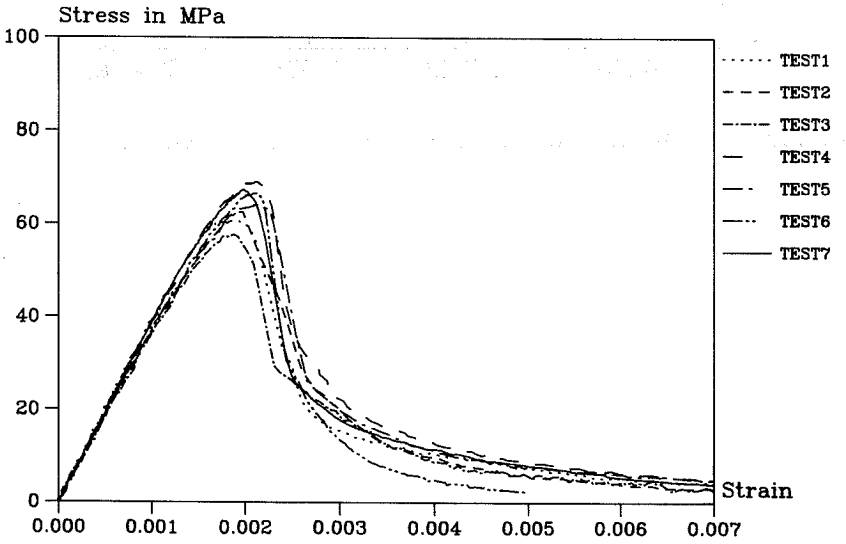

Fig. 4.2 Stress-strain curves of high strength concrete with compressive strength on the of 70 MPa level, from the first test series.

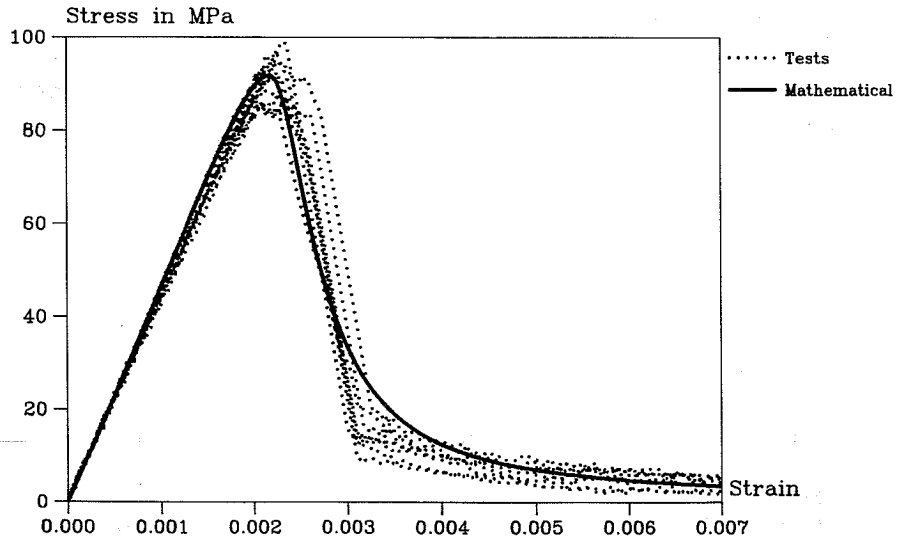

Fig. 4.3 The mathematical fit to the stress-strain curves of high strength concrete with compressive strength on the 90 MPa level, from the first test series.

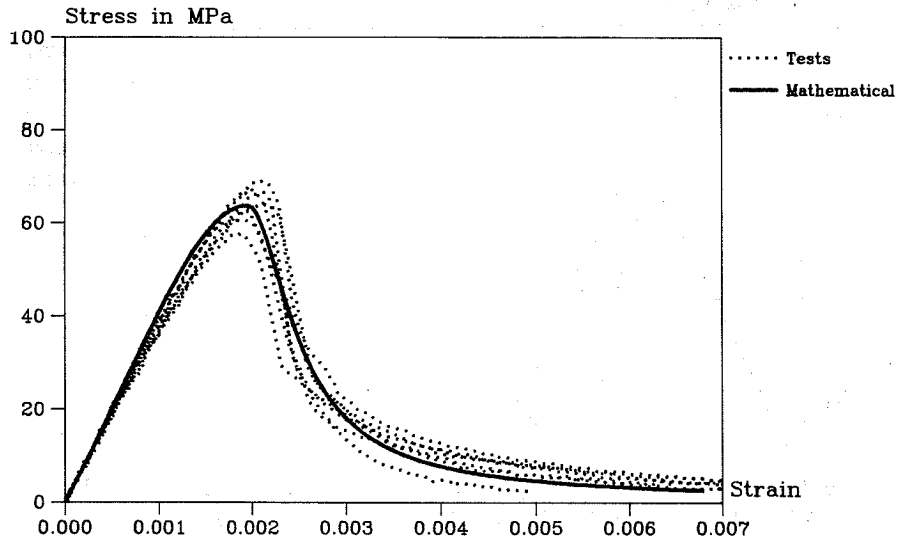

Fig. 4.4 The mathematical fit to the stress-strain curves of high strength concrete with compressive strength on the 70 MPa level, from the first test series.

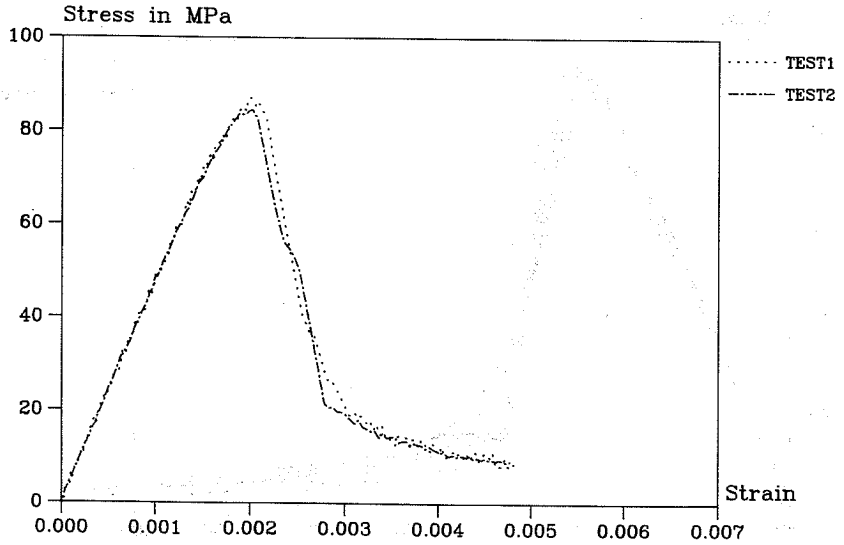

Fig. 5.1 Stress-strain curves of high strength concrete with compressive strength on the 90 MPa level, from the second test series.

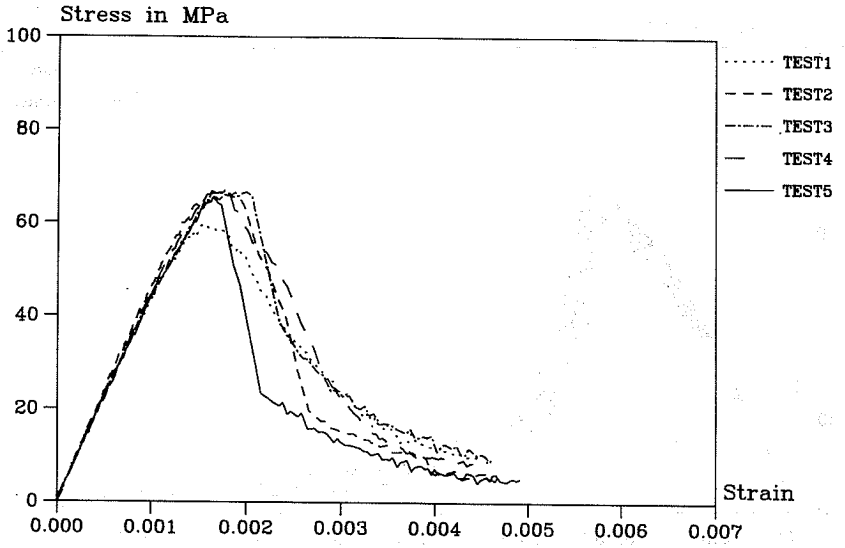

Fig. 5.2 Stress-strain curves of high strength concrete with compressive strength on the 70 MPa level, from the second test series.

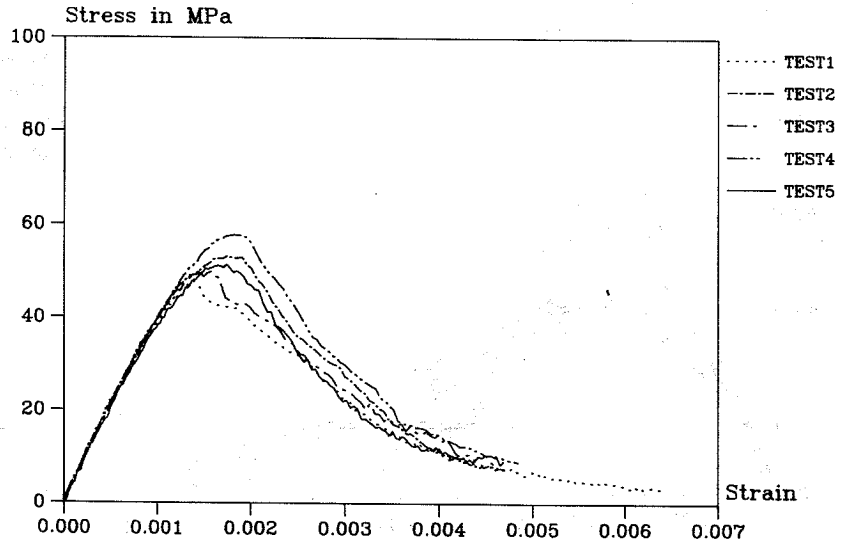

Fig. 5.3 Stress-strain curves of normal strength concrete with compressive strength on the 50 MPa level, from the second test series.

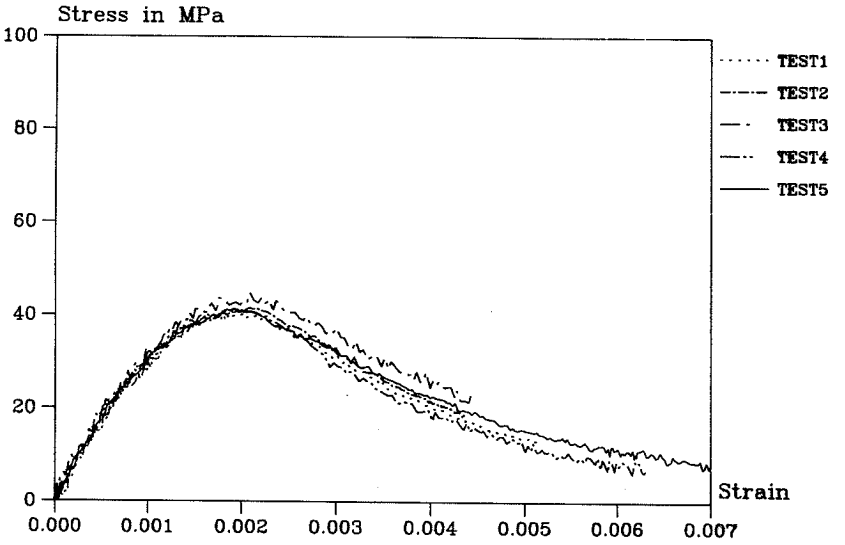

Fig. 5.4 Stress-strain curves of normal strength concrete with compressive strength on the 40 MPa level, from the second test series.

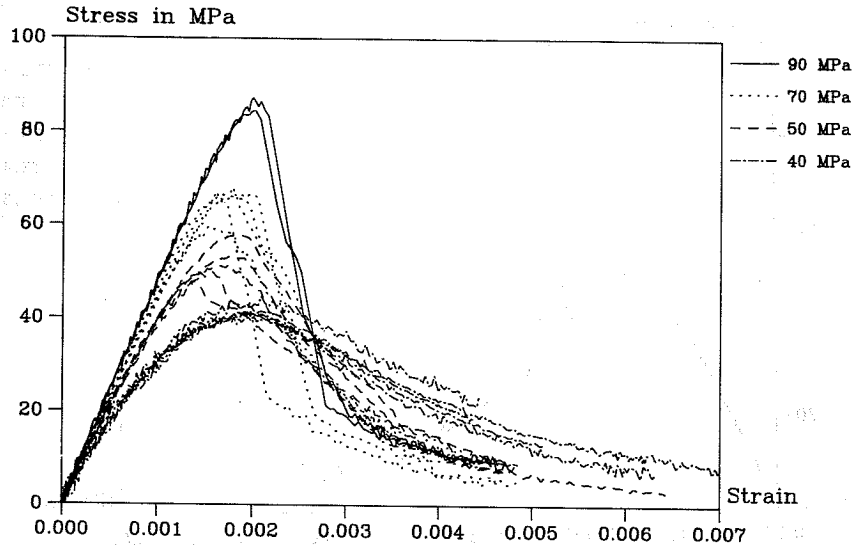

Fig. 5.5 All stress-strain curves from the second test series.

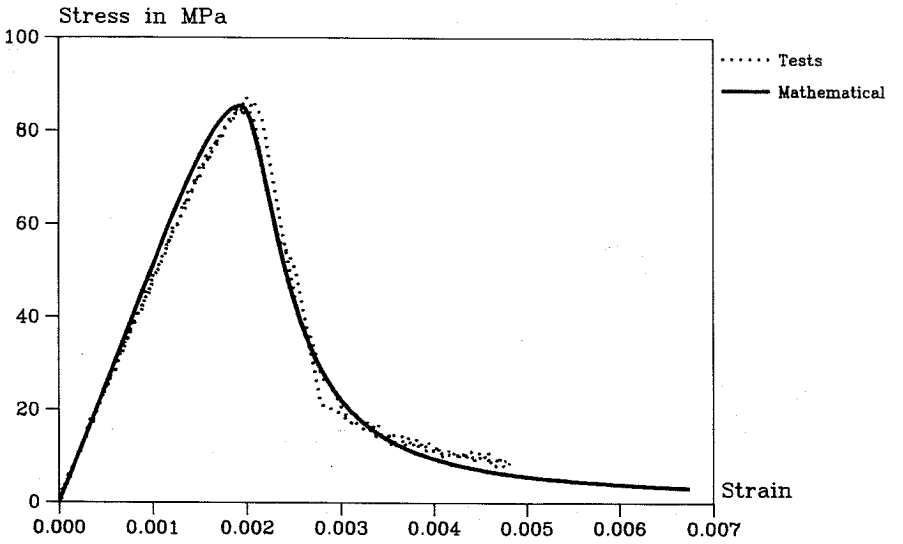

Fig. 5.6 The mathematical fit to the stress strain curves of high strength concrete with compressive strength on the 90 MPa level, from the second test series.

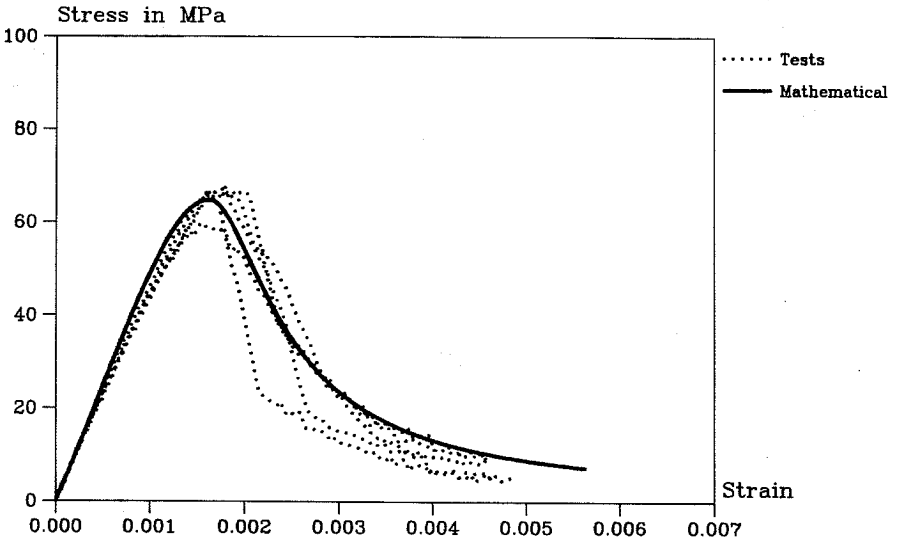

Fig. 5.7 The mathematical fit to the stress strain curves of high strength concrete with compressive strength on the 70 MPa level, from the second test series.

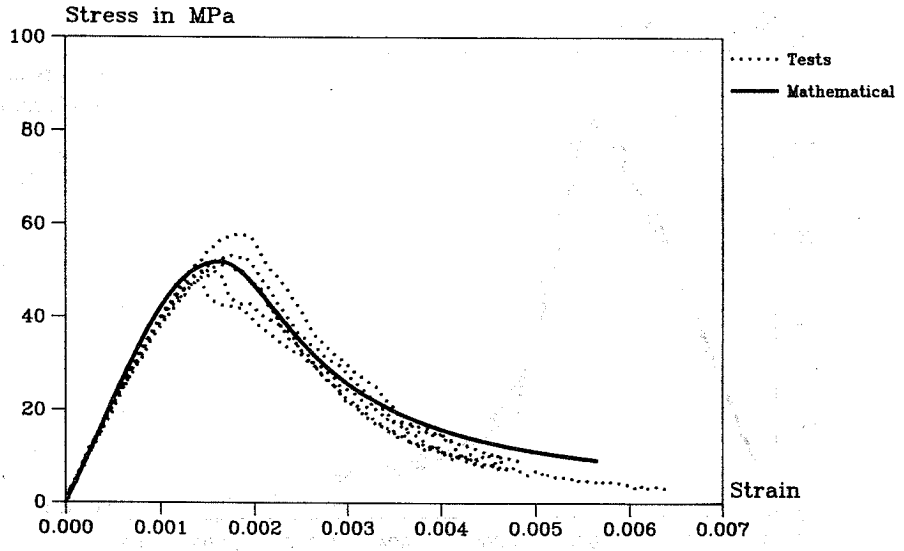

Fig. 5.8 The mathematical fit to the stress strain curves of normal strength concrete with compressive strength on the 50 MPa level, from the second test series.

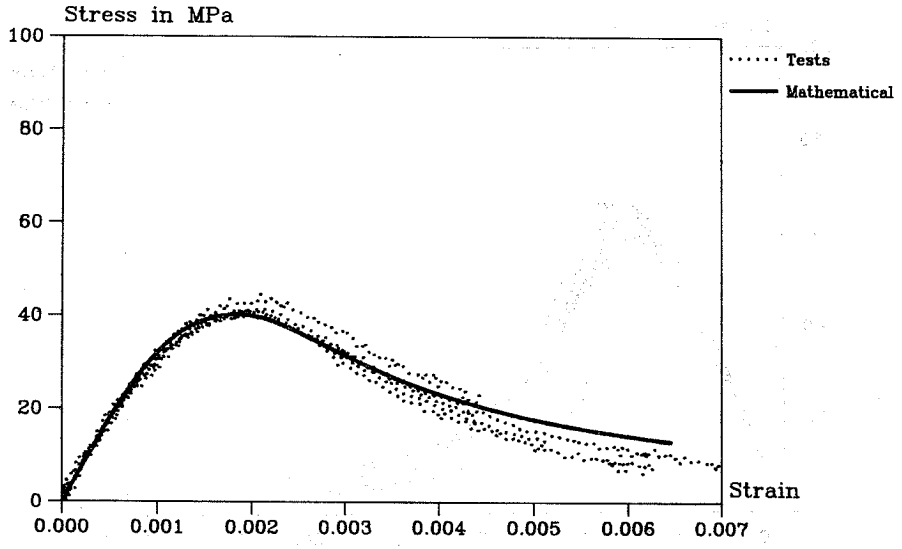

Fig. 5.9 The mathematical fit to the stress strain curves of normal strength concrete with compressive strength on the 40 MPa level, from the second test series.

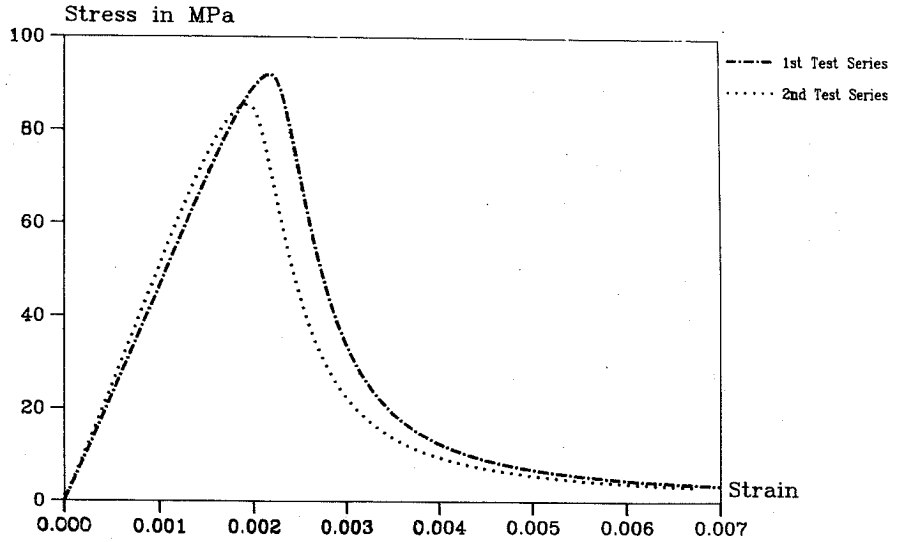

Fig. 5.10 Comparison between mathematical representations of stress strain curves of high strength concrete with compressive strength on the 90 MPa level from the first and second test series.

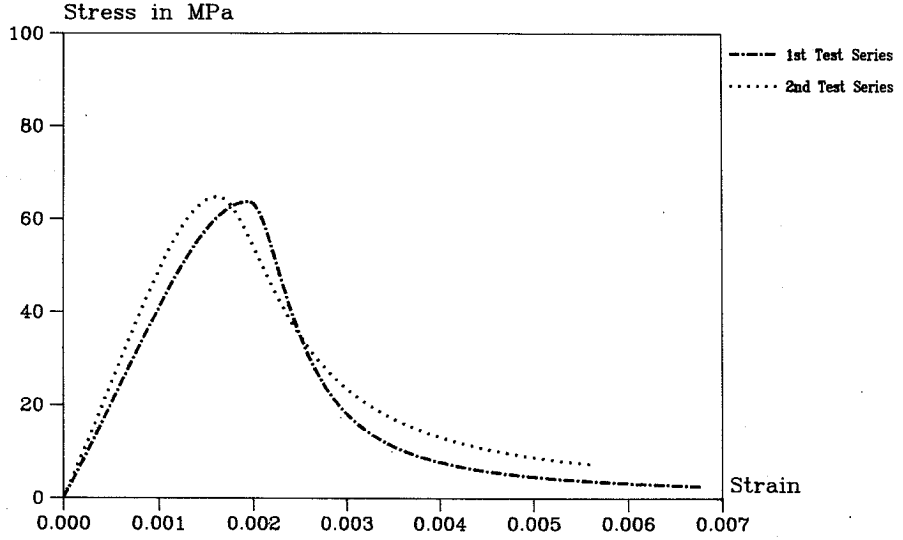

Fig. 5.11 Comparison between mathematical representations of stress strain curves of high strength concrete with compressive strength on the 70 MPa level from the first and second test series.

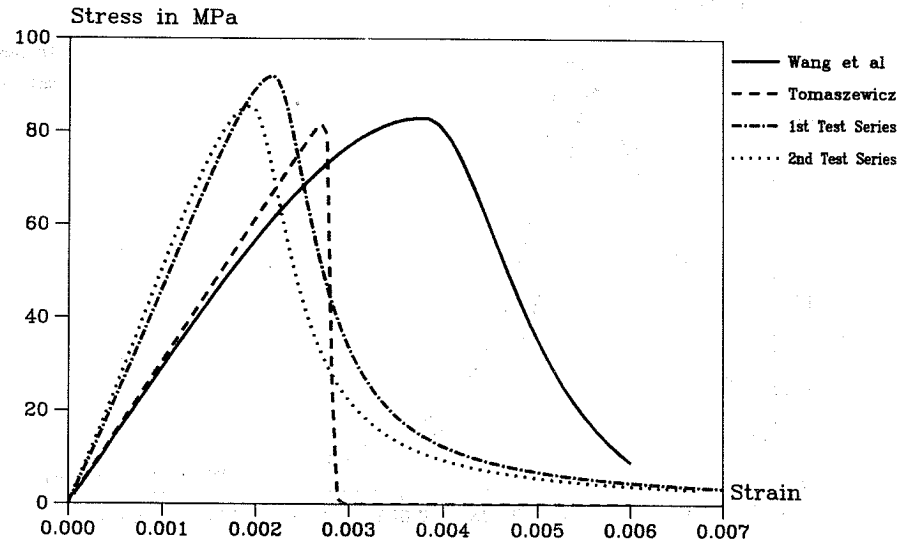

Fig. 6.1 Comparison between mathematical representations of stress strain curves of high strength concrete with compressive strength on the 90 MPa level.

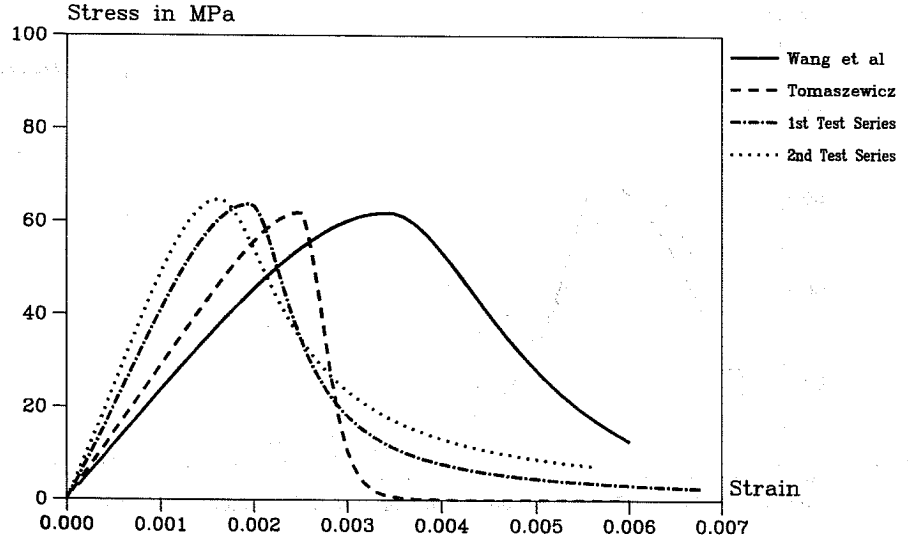

Fig. 6.2 Comparison between mathematical representations of stress strain curves of high strength concrete with compressive strength on the 70 MPa level.

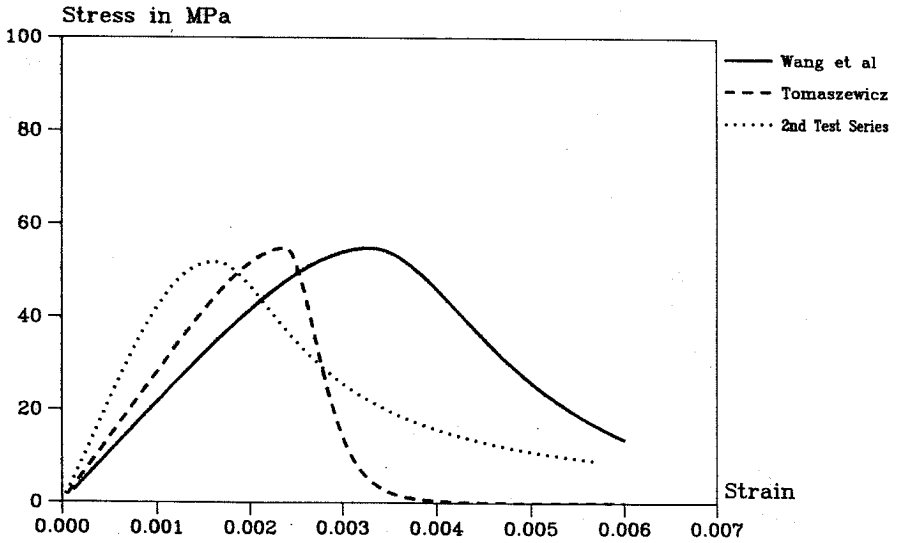

Fig. 6.3 Comparison between mathematical representations of stress strain curves of normal strength concrete with compressive strength on the 50 MPa level.

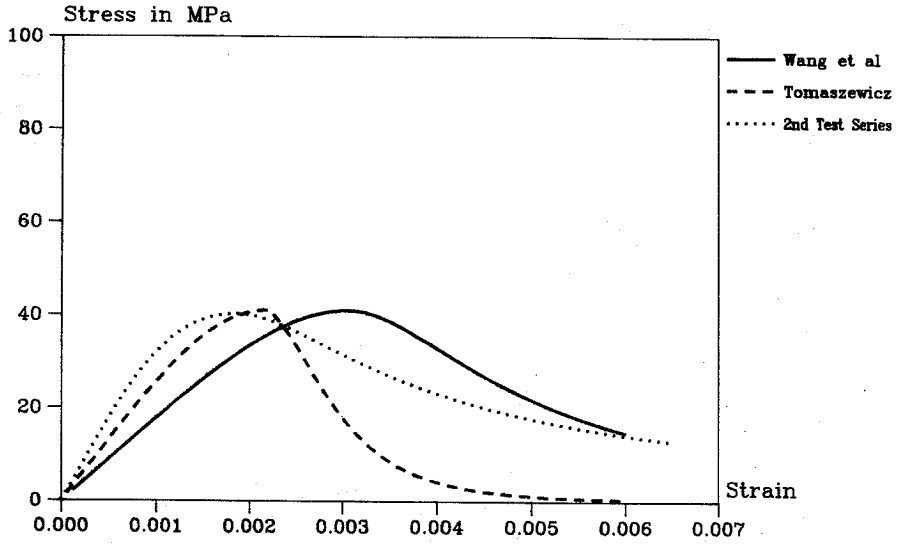

Fig. 6.4 Comparison between mathematical representations of stress strain curves of normal strength concrete with compressive strength on the 40 MPa level.

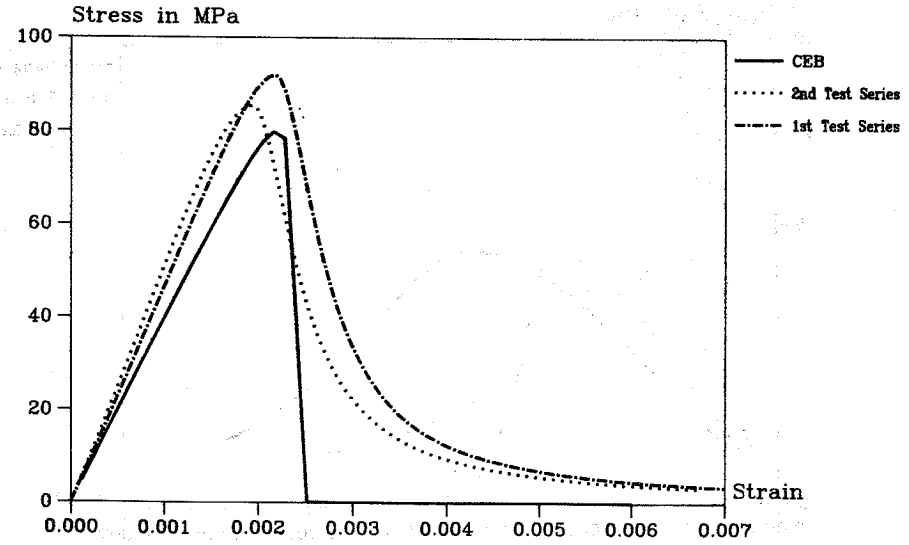

Fig. 6.5 Mathematical representations of stress-strain curves of 90 MPa high strength concrete, compared to mathematical proposal from CEB.

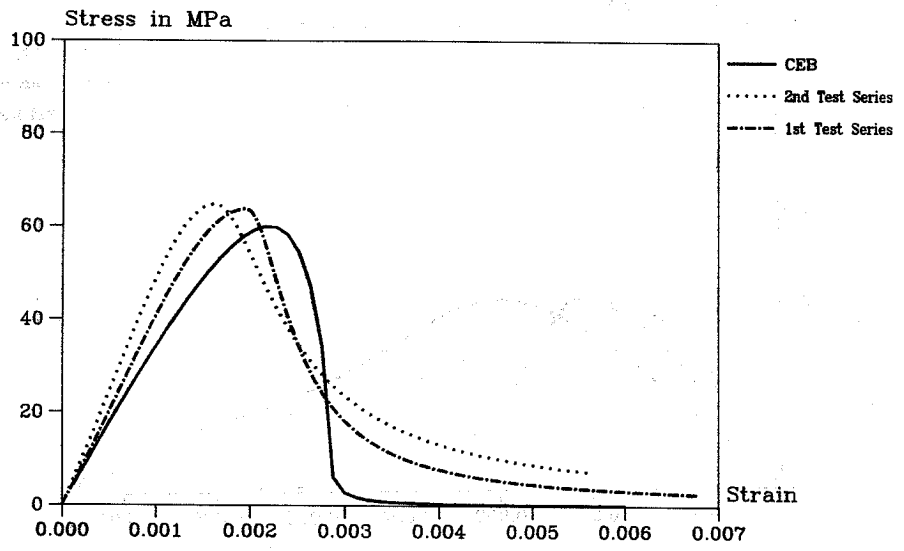

Fig. 6.6 Mathematical representations of stress-strain curves of 70 MPa high strength concrete, compared to mathematical proposal from CEB.

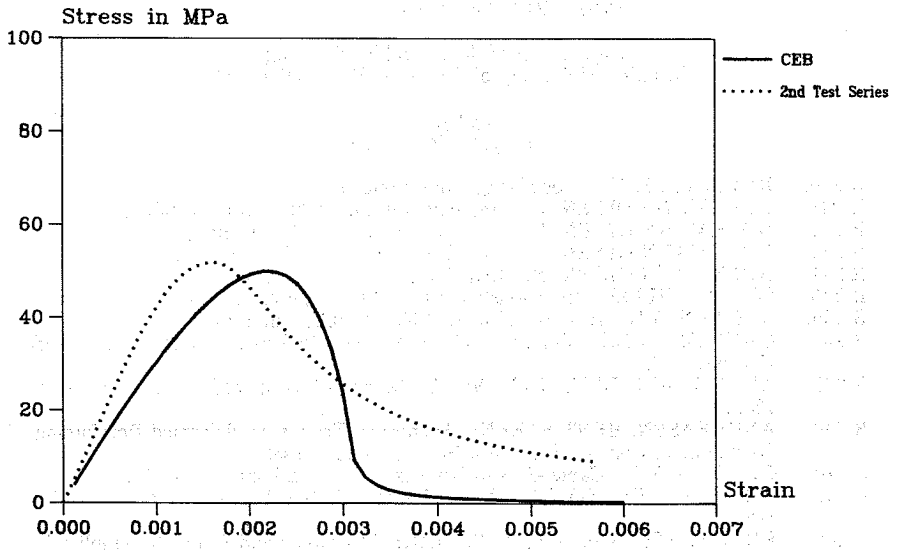

Fig. 6.7 Mathematical representations of stress-strain curves of 50 MPa normal strength concrete, compared to mathematical proposal from CEB.

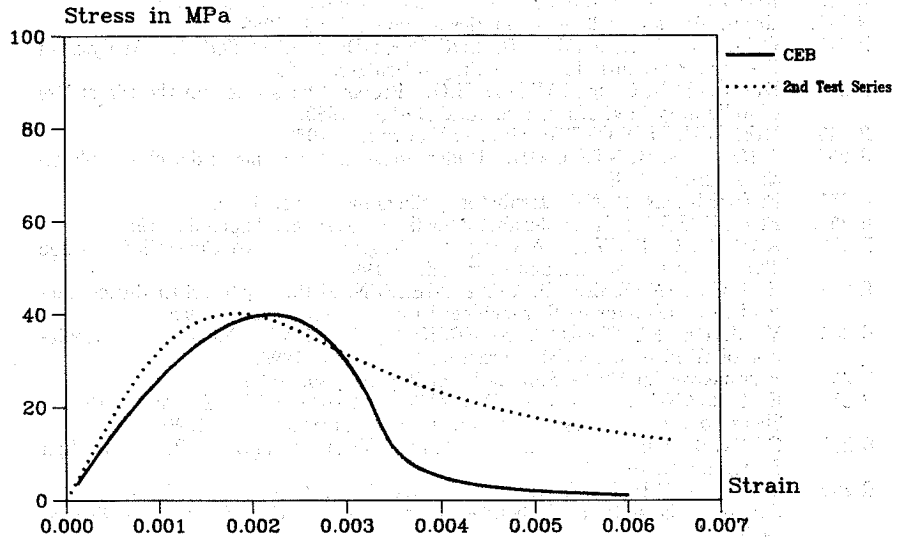

Fig. 6.8 Mathematical representations of stress-strain curves of 40 MPa normal strength concrete, compared to mathematical proposal from CEB.

AFDELINGEN FOR BÆRENDE KONSTRUKTIONER
DANMARKS TEKNISKE HØJSKOLE

Department of Structural Engineering
Technical University of Denmark, DK–2800 Lyngby

SERIE R
(Tidligere: Rapporter)

R 230. RIBERHOLT, H.: Woodflanges under tension, 1988.
R 231. HOLKMANN OLSEN, N.: Implementation. 1988. (public. pending).
R 232. HOLKMANN OLSEN, N.: Uniaxial. 1988. (public pending)
R 233. HOLKMANN OLSEN, N.: Anchorage. 1988. (public pending)
R 234. HOLKMANN OLSEN, N.: Heat Induced. 1988. (public pending)
R 235. SCHEEL, HELLE: Rotationskapacitet. 1988. (public pending)
R 236. NIELSEN, MONA: Arbejdslinier. 1988. (public pending)
R 237. GANWEI, CHEN: Plastic Analysis of Shear in Beams. Deep Beams and Corbels. 1988.
R 238. ANDREASEN, BENT STEEN: Anchorage of Deformed Reinforcing bars. 1988.
R 239. ANDREASEN, BENT STEEN: Anchorage Tests with deformed Reinforcing Bars in more than one layer at a Beam Support. 1988.
R 240. GIMSING, N.J.: Cable–Stayed Bridges with Ultra Long Spans. 1988.
R 241. NIELSEN, LEIF OTTO: En Reissner–Mindlin Plade Element Familie. 1989.
R 242. KRENK, STEEN og THORUP, ERIK: Stochastic and Concrete Amplitude Fatigue Test of Plate Specimens with a Central Hole. 1989.
R 243. AARKROG, P., THORUP, E., KRENK, S., AGERSKOV, H. and BJØRNBAK–HANSEN, J.: Apparatur til Udmattelsesforsøg. 1989.
R 244. DITLEVSEN, OVE and KRENK, STEEN: Research Workshop on Stochastic Mechanics, September 13–14, 1988.
R 245. ROBERTS, J.B.: Averaging Methods in Random Vibration. 1989.
R 246. Resumeoversigt 1988 – Summaries of Papers 1988. 1989.
R 247. GIMSING, N.J., JAMES D. LOCKWOOD, JAEHO SONG: Analysis of Erection Procedures for Cable–Stayed Bridges. 1989.
R 248. DITLEVSEN, O. og MADSEN, H.O.: Proposal for a Code for the Direct Use of Reliability Methods in Structural Design. 1989.
R 249. NIELSEN, LEIF OTTO: Simplex Elementet. 1989.
R 250. THOMSEN, BENTE DAHL: Undersøgelse af "shear lag" i det elasto–plastiske stadium. 1990.
R 251. FEDDERSEN, BENT: Jernbetonbjælkers bæreevne. 1990.
R 252. FEDDERSEN, BENT: Jernbetonbjælkers bæreevne, Appendix. 1990.
R 253. AARKROG, PETER: A Computer Program for Servo Controlled Fatigue Testing Documentation and User Guide. 1990.
R 254. HOLKMANN OLSEN, DAVID & NIELSEN, M.P.: Ny Teori til Bestemmelse af Revneafstande og Revnevidder i Betonkonstruktioner. 1990.
R 255. YAMADA, KENTARO & AGERSKOV, HENNING: Fatigue Life Prediction of Welded Joints Using Fracture Mechanics. 1990.
R 256. Resumeoversigt 1989 – Summaries of Papers 1989. 1990.
R 257. HOLKMANN OLSEN, DAVID, GANWEI, CHEN, NIELSEN, M.P.: Plastic Shear Solutions of Prestressed Hollow Core Concrete Slabs. 1990.
R 258. GANWEI, CHEN & NIELSEN, M.P.: Shear Strength of Beams of High Strength Concrete. 1990.
R 259. GANWEI, CHEN, NIELSEN, M.P. NIELSEN, JANOS, K.: Ultimate Load Carrying Capacity of Unbonded Prestressed Reinforced Concrete Beams. 1990.
R 260. GANWEI, CHEN, NIELSEN, M.P.: A Short Note on Plastic Shear Solutions of Reinforced Concrete Columbs. 1990.
R 261. GLUVER, HENRIK: One Step Markov Model for Extremes of Gaussian Processes. 1990.

Abonnement 1.7.1990 – 30.6.1991 kr. 130,–
Subscription rate 1.7.1990 – 30.6.1991 D.Kr. 130.–.

Hvis De ikke allerede modtager Afdelingens resumeoversigt ved udgivelsen, kan Afdelingen tilbyde at tilsende næste års resumeoversigt, når den udgives, dersom De udfylder og returnerer nedenstående kupon.

Returneres til
Afdelingen for Bærende Konstruktioner
Danmarks tekniske Højskole
Bygning 118
2800 Lyngby

Fremtidig tilsendelse af resumeoversigter udbedes af
(bedes udfyldt med blokbogstaver):

Stilling og navn: .....

Adresse: .....

Postnr. og -distrikt: .....

The Department has pleasure in offering to send you a next year's list of summaries, free of charge. If you do not already receive it upon publication, kindly complete and return the coupon below.

To be returned to:
Department of Structural Engineering
Technical University of Denmark
Building 118
DK-2800 Lyngby, Denmark.

The undersigned wishes to receive the Department's
List of Summaries:
(Please complete in block letters)

Title and name .....

Address.....

Postal No. and district.....

Country.....